Inner-shell ionization cross sections for PIXE quantitative analysis

Author: Pau Fité López, pfitelop16@alumnes.ub.edu
Facultat de Física, Universitat de Barcelona, Diagonal 645, ES-08028 Barcelona, Spain

Advisor: José M. Fernández-Varea, jm.fernandezvarea@ub.edu
(Dated: June 13, 2025)

Abstract: The aim of this Final Degree Project is to study two models for the inner-shell ionization cross sections by light-ion impact. One is the plane-wave Born approximation (PWBA). The other is the eCPSShsR model, which improves the PWBA including the Coulomb, binding and wave function corrections. Numerical calculations have been done for Al, Cu, and Ag atoms, and H^+ and He^{2+} ions with energies from 0.05 MeV to 20 MeV. The comparison of the theoretical predictions with experimental data shows that the eCPSShsR approximation is quite accurate and that, for large projectile energies, the PWBA and eCPSShsR models are nearly identical.
Keywords: Cross section, ionization, x-ray, screening, inelastic collision, corrections.
SDGs: Quality education. Industry, innovation, infrastructure.

I. INTRODUCTION

Atomic ionization caused by the impact of charged particles is a fundamental process in nature. The interaction between charged particles such as H^+ or He^{2+} ions and atoms can lead to the ejection of electrons from the inner atomic (sub)shells, creating vacancies. These holes are often filled with electrons from outer shells, emitting characteristic x rays. The family of techniques that studies these interactions is called Ion Beam Analysis (IBA), the most important being particle-induced x-ray emission (PIXE) due to its high sensitivity and its non-destructive nature.

In PIXE, proton beams of 1–5 MeV are frequently used to excite the atoms of a sample. The electronic transitions following the ionization of K-shell or L-subshell electrons produce characteristic x-rays. Detecting the energy of this radiation, the composition of the irradiated material can be derived [1]. This has many implications in different fields such as materials science, biology or even art.

In the following sections we outline the calculation of K-shell ionization cross section for non-relativistic bare ions. To model this process, we employ the plane-wave Born approximation (PWBA), which provides a theoretical framework to describe electron ejection in inelastic collisions. This formalism will allow us to calculate cross sections for the direct ionization of atomic shells by light-ion impact.

II. THEORETICAL FRAMEWORK

A. Plane-wave Born approximation

In the PWBA the inelastic collision of the projectile and the target is described using quantum mechanics. The wave function of the projectile before and after the collision is a plane wave. If the charge of the projectile is small compared to that of the target atom, the interaction between them can be treated as a 1st-order perturbation [2].

The projectile is defined by its charge $Z_1 e$ (e is the elementary charge) and mass M_1. It moves at an initial velocity v_1 and its kinetic energy is $E_1 = \frac{1}{2} M_1 v_1^2$. The target has charge $Z_2 e$ and mass M_2 and is initially at rest. The collision is characterised by an energy transfer $W \equiv E_1 - E_1'$ and a momentum transfer $\vec{\mathbf{q}} \equiv \vec{\mathbf{p}}_1 - \vec{\mathbf{p}}\,'_1$, where the prime refers to the values of the magnitudes of the projectile after the collision. These are measured in the laboratory reference frame (LRF). As we will consider $M_2 < \infty$, it is necessary to define the reduced mass M and the energy E in the centre-of-mass reference frame (CMRF). Since for non-relativistic projectiles the relative velocity is frame independent, the following relation is valid: $E = ME_1/M_1$. Therefore, the energy in the CMRF is $E = \frac{1}{2} M v^2$. To deduce an expression for the integrated cross section (ICS), it is useful to work with the recoil energy $Q \equiv q^2/(2m_\mathrm{e})$ (m_e is the electron rest mass), which represents the kinetic energy that a free, stationary electron would acquire if a linear momentum $\vec{\mathbf{q}}$ were transferred to it.

The Fermi golden rule yields the doubly differential cross section (DDCS) for K-shell ionization [2]

$$\frac{\mathrm{d}^2\sigma_\mathrm{K}}{\mathrm{d}W\,\mathrm{d}Q} = \frac{2\pi Z_1^2 e^4}{m_\mathrm{e} v_1^2} \frac{1}{WQ} \frac{\mathrm{d}f_\mathrm{K}(Q,W)}{\mathrm{d}W} \ , \qquad (1)$$

where $\mathrm{d}f_\mathrm{K}/\mathrm{d}W$ is the generalized oscillator strength (GOS), which is closely related to the inelastic form factor. The latter is the matrix element of the ion-atom Coulomb interaction between the initial and final states of the unperturbed system [2]. As mentioned above, plane waves are used to describe the projectile. To avoid the complexities of the numerical evaluation of the GOS, here we adopt the analytical GOS pertaining to a Coulomb potential. In the case of the K shell, the initial wave function of the active electron is a hydrogenic 1s orbital with an effective charge $Z_{2\mathrm{K}} = Z_2 - 0.3$ to account for inner screening. The corresponding expression of the

GOS is shown in Ref. [3] and Appendix A. A more rigorous approach would require relativistic wave functions and the GOS would not be analytical.

To obtain the ICS, the DDCS has to be integrated twice,

$$\sigma_{\mathrm{K}} = \int_{W_{\min}}^{W_{\max}} \mathrm{d}W \int_{Q_-}^{Q_+} \mathrm{d}Q \; \frac{\mathrm{d}^2\sigma_{\mathrm{K}}}{\mathrm{d}W \; \mathrm{d}Q} \; . \tag{2}$$

The limits of the integral over W are given by the minimum energy transfer (experimental ionization energy U_{K} to account for outer screening) and the maximum energy transfer E. The limits of the Q integral follow from the condition of minimum ($\theta = 0°$) and maximum ($\theta = 180°$) momentum transfers, q_- and q_+, respectively. Specifically,

$$W_{\min} = U_{\mathrm{K}}, \qquad W_{\max} = E, \tag{3}$$

$$Q_{\pm}(W) = \frac{q_{\pm}^2}{2m_{\mathrm{e}}} = \frac{M}{m_{\mathrm{e}}} E \left[1 \pm \sqrt{1 - \frac{W}{E}}\right]^2 . \tag{4}$$

When the integral is evaluated with these limits, the result is known as the "exact" PWBA (ePWBA). In the older literature, most of the authors used the approximate adiabatic limits $W_{\max} = Q_+ = \infty$; this simplification was called "standard" PWBA.

Another historically relevant approximation is the one developed by Huus, Bjerregaard and Elbek in 1956 [4] which is applicable for collisions where $Q \gg W$, being thus well suited to describe the ICS for low values of E_1. It can be obtained with a Taylor expansion of the GOS expression, yielding

$$\mathrm{d}f_{\mathrm{K}}(Q,W)/\,\mathrm{d}W \approx 2^5 \left(Z_{2\mathrm{K}}^2 E_{\mathrm{h}}\right)^3 W Q^{-5} \; , \tag{5}$$

where E_{h} is the Hartree energy. Then, adopting the adiabatic integration limits in Eq. (2), the result is

$$\sigma_{\mathrm{K}}^{\mathrm{HBE}} = \frac{2^{24}\,\pi}{3^2 \cdot 5} \frac{Z_1^2 e^4}{Z_{2\mathrm{K}}^{12}} \frac{1}{E_{\mathrm{h}}^6} \left(\frac{m_{\mathrm{e}} E_1}{M_1}\right)^4 , \tag{6}$$

which is strongly dependent on $Z_{2\mathrm{K}}$ and E_1.

B. Corrections to the PWBA

The limitations of the PWBA become apparent when trying to describe the ionization ICS for low-energy projectiles. Three corrections can be implemented to improve the performance of the PWBA. To do so, it is necessary to introduce a reduced variable used in the literature on this topic that will appear in all corrections [2]

$$\xi_{\mathrm{K}} = \sqrt{2 Z_{2\mathrm{K}}^2 \frac{m_{\mathrm{e}}}{M_1} \frac{E_1 E_{\mathrm{h}}}{U_{\mathrm{K}}^2}} \; . \tag{7}$$

Coulomb correction: the Coulomb correction takes into account that, for low projectile energies, the nucleus of the target atom deflects the trajectory of the projectile, making it hyperbolic. This causes a decrease of the ICS. To attain a mathematical expression for this correction, it is reasonable to work with another formalism called the semi-classical approximation (SCA), which considers a classical projectile that follows a well-defined trajectory and a quantum-mechanically described electron target.

This correction takes form of a multiplicative factor equal to the ratio between the ICSs of the hyperbolic (hyp) and straight-line (str) trajectories,

$$\sigma_{\mathrm{K}}^{\mathrm{C}} = C_{\mathrm{K}} \, \sigma_{\mathrm{K}}^{\mathrm{ePWBA}} \; , \tag{8}$$

$$C_{\mathrm{K}} \equiv \sigma_{\mathrm{K}}^{\mathrm{SCA,hyp}} / \sigma_{\mathrm{K}}^{\mathrm{SCA,str}} = 9\, E_{10}(\pi d q_{0\mathrm{K}}/\hbar) \; , \tag{9}$$

where $E_n(x)$ is the exponential integral of order n, d is half of the minimum distance between the projectile and the target nucleus when $b = 0$ (being b the impact parameter), $q_{0\mathrm{K}} \equiv U_{\mathrm{K}}/v_1$ and $\hbar$ is the reduced Planck constant [2]. The derivation of the expression for C_{K} can be found in Appendix B.

Binding correction: in the low projectile energy regime, large Q values are being considered. Consequently, b is expected to be very small ($b\,q \sim \hbar$), which means that the projectile penetrates deep into the electron cloud. By Gauss' theorem, when the projectile is close to the target nucleus, the effective charge that the active electron feels is $Z_1 + Z_2$, thus increasing its binding energy. There are two main paths to take this physical situation into account, the first of which is called perturbed stationary state correction (PSS). The idea is that, if the binding energy increases, the lower limit of the integral in W will be shifted to $U_{\mathrm{K}} + \langle \Delta U_{\mathrm{K}} \rangle \leq W \leq E$, where $\langle \Delta U_{\mathrm{K}} \rangle$ can be calculated as

$$\langle \Delta U_{\mathrm{K}} \rangle = \int_0^{c_{\mathrm{K}}/\xi_{\mathrm{K}}} \Delta U_{\mathrm{K}}(\xi_{\mathrm{K}} x)\, w_{\mathrm{K}}(x) \; \mathrm{d}x \; , \tag{10}$$

with $c_{\mathrm{K}} = 3/2$, $w_{\mathrm{K}}(x) = 5x^4 K_2^2(x)/32$ is a weight function and $K_2(x)$ is the modified Bessel function [2]. A rigorous derivation of ΔU_{K} is given in Appendix C.

The other approach was developed by Anholt and Meyerhof [5] and it is introduced in the PWBA ICS through a multiplicative factor B_{K}. Their disquisition was: when the projectile comes very close to the nucleus, the K-shell electron has a binding energy similar to that of an electron in the K shell of an atom with atomic number $Z_2 + Z_1$, i.e. $U_{\mathrm{K}}^{\mathrm{UA}} = U_{\mathrm{K}}(Z_2 + Z_1)$, where UA stands for "united atom". Then, B_{K} becomes

$$B_{\mathrm{K}} = \left(U_{\mathrm{K}}/U_{\mathrm{K}}^{\mathrm{UA}}\right)^{n(\xi_{\mathrm{K}})} \; , \tag{11}$$

where $n(\xi_{\mathrm{K}})$ is an empirical function found in the article above. It is introduced to the ICS with a factor as in Eq. (8).

Wave function correction: the wave function correction has a double purpose. It introduces the fact that, when the projectile is close to the nucleus of the target atom, a relativistic and non-hydrogenic description

of the target is better suited (the GOS is relativistic and not analytical).

The mathematical expression of this correction is also through a multiplicative factor

$$W_{\mathrm{K}}^{\mathrm{hsR}}(\xi_{\mathrm{K}}, Z_2) = \exp\Big\{A(Z_2)/\xi_{\mathrm{K}} - B(Z_2)/\xi_{\mathrm{K}}^2 + C(Z_2)/\xi_{\mathrm{K}}^3 - D(Z_2)/\xi_{\mathrm{K}}^4\Big\} \ . \quad (12)$$

The derivation of this correction can be found in Ref. [6], which was calculated using Dirac–Hartree–Slater wave functions. It is introduced in the ICS as in Eq. (8).

If we want to combine all three corrections together, we would have to replace in Eq. (7) U_{K} with $U_{\mathrm{K}} + \langle \Delta U_{\mathrm{K}} \rangle$. In this work's case, we have incorporated the Coulomb factor, the PSS correction and the wave function factor in the ePWBA ICS, which we call eCPSShsR

$$\sigma_{\mathrm{K}}^{\mathrm{eCPSShsR}} = W_{\mathrm{K}}^{\mathrm{hsR}}\, C_{\mathrm{K}}\, \sigma_{\mathrm{K}}^{\mathrm{ePSS}} \ . \quad (13)$$

C. Numerical implementation

To compute the K-shell ionization ICSs I have developed a Fortran 90 code that calculates the double integral in Eq. (2) with Simpson's rule. I have defined a function $F(W)$ as the integral over Q and then integrated it over W. Because large values of Q and W contribute to the integral, it is convenient to employ the variables $\ln Q$ and $\ln W$. The values of $A_1(\mathcal{Q}, \mathcal{W})$ factor in Eq. (A4) are calculated with the Fortran function `ATAN2(Y,X)`. It computes the principal value of the argument function of the complex number $X + \mathrm{i}Y$, this was used in order to clearly state the quadrant of the argument of the arctangent and avoid ambiguities. Simpson's rule was also used in the evaluation of the PSS correction, Eq. (10). For $E_n(x)$ in Eq. (9) and $K_2(x)$ in Eq. (10) I applied the expansions found in Ref. [7].

III. RESULTS AND DISCUSSION

A. Cross section model analysis

The experimental articles on this topic usually give the value for the x-ray production ICS $\sigma_{\mathrm{K}}^{\mathrm{x}}$. To convert the values to the K-shell ICS, the following relationship is needed:

$$\sigma_{\mathrm{K}} = \sigma_{\mathrm{K}}^{\mathrm{x}}/\omega_{\mathrm{K}} \ , \quad (14)$$

where ω_{K} is the K-shell fluorescence yield, i.e. the probability that a hole in the K-shell is filled by a radiative process in competition with non-radiative processes (Auger effect). The values for ω_{K} were taken from Ref. [8].

The articles from which the experimental $\sigma_{\mathrm{K}}^{\mathrm{x}}$ are taken are listed in Appendix D.

In Fig. 1 it is noticeable that the K-shell ionization ICS exhibits a clear inverse relationship with the atomic number of the target element. The ordinate axis reveals that as the proton count increases, the ICS decreases significantly. The curve migrates towards the right-hand side of the abscissa as Z_2 increases, which points in the same direction of the previous argument.

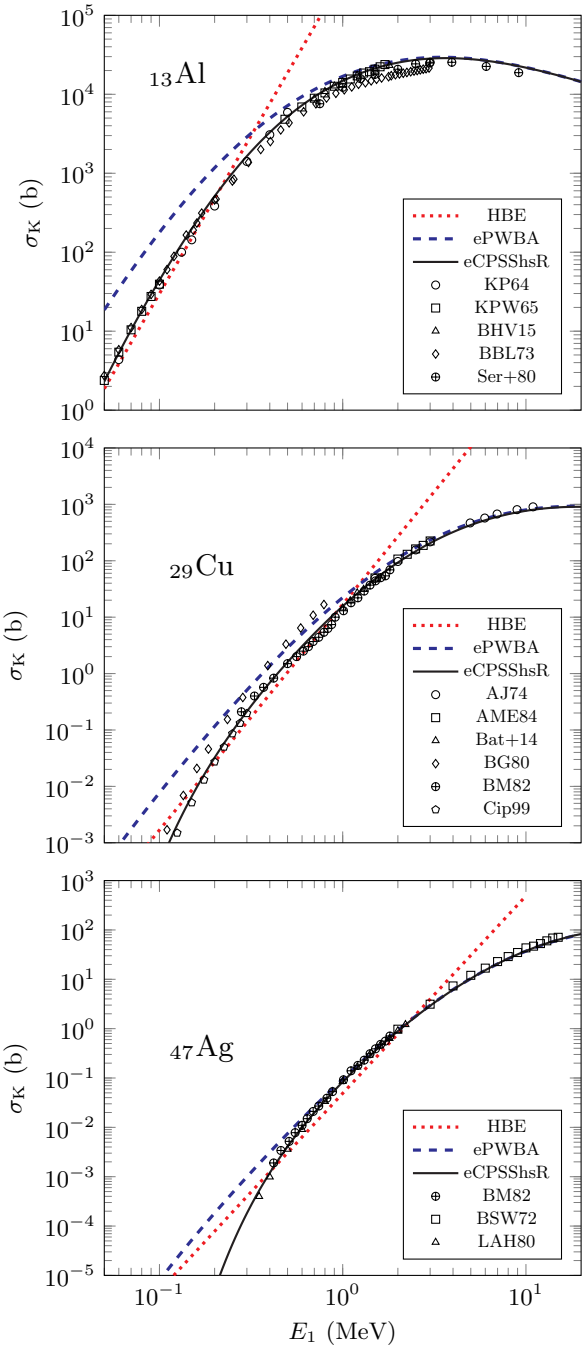

FIG. 1: Al-K, Cu-K, and Ag-K ionization ICSs for the impact of H^+ ions. The curves were calculated with the HBE, ePWBA, and eCPSShsR models. The symbols are experimental data (see Appendix D).

The HBE approximation works reasonably for a narrow interval of E_1, which satisfies $Q \gg W$. Other than

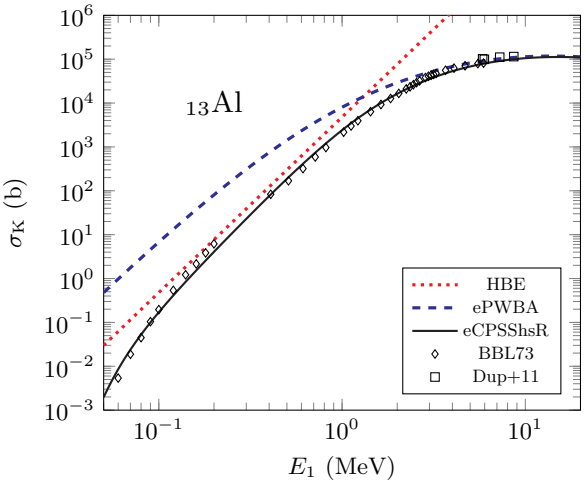

FIG. 2: Al-K ionization ICS for the impact of He^{2+} ions. The curves were calculated with the HBE, ePWBA, and eCPSSShsR models. The symbols are experimental data (see Appendix D).

this sector, the HBE ICS fails to predict the behavior at high and very low projectile energies. For large values of E_1 the ePWBA and the eCPSSShsR are nearly the same curve, with only a minor correction. However, for low E_1, the two plots diverge significantly.

As noted in the previous section, the corrections are most important for low energies, due to the fact that when the collision is "slow" the target and the projectile have "more time" to interact with each other and then the plane-wave assumption is less accurate. Also, the eCPSSShsR modification becomes increasingly important for higher Z_2. Overall, the corrections lower the ICS in comparison to the ePWBA model.

In Fig. 2 it can be seen that a larger Z_1 value magnifies the divergence of the ePWBA and eCPSSShsR models. It can also be mentioned that, for projectiles with larger Z_1, σ_K decreases rapidly for small E_1 values. The curve of the eCPSSShsR model remains in good concordance with the experimental data.

B. eCPSSShsR correction factors analysis

In Fig. 3 the factors are depicted with more detail. The factors plotted are the same as expressed in Eqs. (9), (11), and (12) and calculated without combining the binding correction, that is, with the expression of ξ_K from Eq. (7). The PSS factor has been calculated as $\sigma_K^{ePSS}/\sigma_K^{ePWBA}$, so it would be an 'effective factor'.

It is clear that many of the arguments exposed above are corroborated with these images too. For instance, the Coulomb factor grows in importance (becomes closer to zero) when the charge of the target is larger, which is understandable because the repulsion of both positively-charged particles becomes stronger.

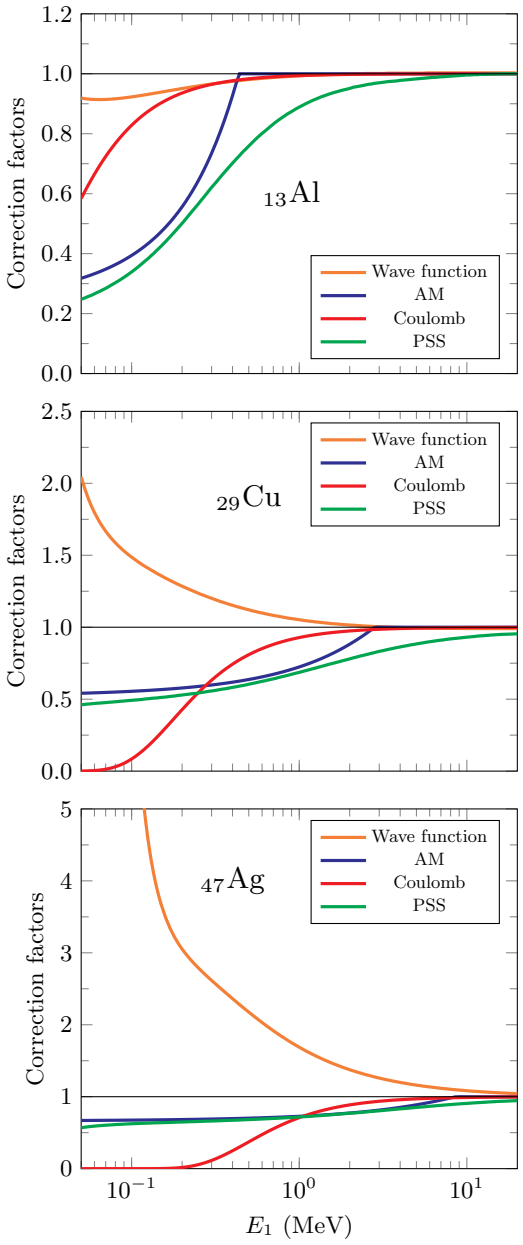

FIG. 3: Correction factors implemented in the eCPSSShsR model (Coulomb, PSS, AM —Anholt and Meyerhof's— and wave function) as a function of projectile energy for Al, Cu, and Ag targets and H^+ projectile.

Taking a look at the binding corrections, it is remarkable that both approximations are really similar, but the PSS factor may be more useful for further calculations because it is differentiable. The 'strange' behavior of the AM factor is due to the definition of $n(\xi_K)$ in Eq. (11), which is a piecewise function. For small Z_2 atoms the binding factors decrease the ICS in a very intense way but it converges quite fast to one when increasing E_1. On the other hand, the binding factors are not that im-

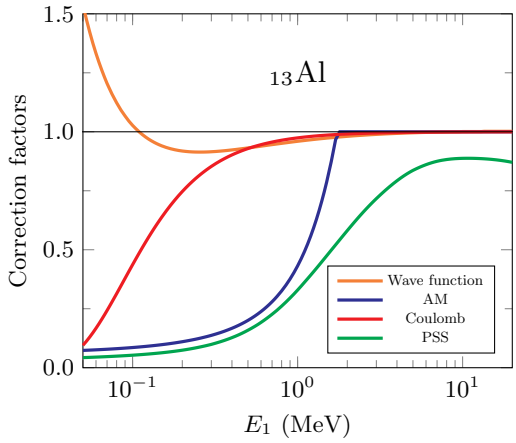

FIG. 4: Correction factors implemented in the eCPSShsR model (Coulomb, PSS, AM —Anholt and Meyerhof's— and wave function) as a function of projectile energy for Al target and He^{2+} projectile.

portant for large Z_2 but they tend to converge to one slower.

The wave function factor exhibits a peculiar characteristic: it is smaller than one for Al and it is bigger than one for Cu and Ag. This trait occurs because the wave function factor corrects two things at once: the non-hydrogenic essence of the interaction between the K-shell active electron and the nucleus for large Z_2 and the need for a relativistic description of the wave function. The hydrogenic 1s reduced radial wave function near the nucleus is $P(r) \propto r$. In the relativistic case, the wave function that comes from the Dirac equation has a larger probability density when $r \to 0$ because the $1s_{1/2}$ large and small reduced radial wave functions $P(r), Q(r) \propto r^{\lambda}$ with $\lambda = \sqrt{1-(\alpha Z)^2} < 1$ (α is the fine-structure constant). Hence, the correction factor must be greater than 1.

For Al, this relativistic description is not that important, for the non-hydrogenic contribution, and in particular the effect of the outer-screening dominates.

It has been said that this is taken into account when considering the experimental ionization energy for the lower value of W and not the hydrogenic value but the wave function correction goes a step further and changes the value of the ICS due to a deformation on the active electron wave function and its deviation from the hydrogenic regime due to a screening of the Coulomb potential caused by spectator electrons.

In Fig. 4, one can acknowledge all the traits that have been displayed in this subsection and realize that larger Z_1 enhances the natural behavior of each correction, that is, binding and Coulomb corrections become more intense and the wave function correction becomes larger or smaller than one depending on which physical phenomena takes the lead.

IV. CONCLUSIONS

The PWBA is a good approach for intermediate values of E_1, large enough values so that the corrections are not important but small enough in order not to have to consider a relativistic projectile.

Moreover, the corrections of the eCPSShsR model prove to be reliable at low projectile energies, and the strong concordance between experimental data and the model curve indicates that these factors capture the fundamental physical processes with reasonable accuracy. The binding and Coulomb corrections tend to decrease the ICS and the contribution of the wave function correction depends on which of the two phenomena (non-hydrogenic or relativistic) is most important. Overall, the eCPSShsR approximation makes the ePWBA ICS smaller. It is also clear that PSS is most important for low Z_2 and C_K and W_K^{hsR} for high Z_2.

ACKNOWLEDGEMENTS

I want to thank the effort and guidance of José María throughout the whole project. With his help, he has made this experience truly enriching and fulfilling. I also want to thank my parents, my colleagues and my girlfriend, their support has brought me this far.

[1] P. A. Mandò. *PIXE (Particle-Induced X-ray Emission)*. In: Encyclopedia of Analytical Chemistry. John Wiley & Sons, 2006.

[2] T. Mukoyama. Inner-shell ionization by light-ion impact. *International Journal of PIXE*, 1(3):209–239, 1991.

[3] S. Heredia-Avalos, R. García-Molina, J. M. Fernández-Varea, I. Abril. Calculated energy loss of swift He, Li, B, and N ions in SiO_2, Al_2O_3, and ZrO_2. *Physical Review A*, 72(5):052902, 2005.

[4] T. Huus, J. H. Bjerregaard, B. Elbek. Measurements of conversion electrons from Coulomb excitation of the elements in the rare earth region. *Matematisk-fysiske Meddelelser*, 30(17), 1956.

[5] R. Anhold. Electronic relativistic and Coulomb deflection effects on a $1s\sigma$-vacancy production. *Physical Review A*, 17(3):983–997, 1978.

[6] G. Lapicki. The status of theoretical K-shell ionization cross sections by protons. *X-Ray Spectrometry*, 34:269–278, 2005.

[7] M. Abramowitz, I. A. Stegun. *Handbook of Mathematical Functions with Formulas, Graphs, and Mathematical Tables*, volume 55. US Government Printing Office, 1972.

[8] M. O. Krause. Atomic radiative and radiationless yields for K and L shells. *Journal of Physical and Chemical Reference Data*, 8(2):307–327, 1979.

[9] W. Brandt, G. Lapicki. Energy-loss effect in inner-shell coulomb ionization by heavy charged particles. *Physical Review A*, 23(4):1717–1729, 1981.

Anàlisi quantitativa de la secció eficaç d'ionització de les capes interiors per PIXE

Author: Pau Fité López, pfitelop16@alumnes.ub.edu
Facultat de Física, Universitat de Barcelona, Diagonal 645, ES-08028 Barcelona, Spain

Advisor: José M. Fernández-Varea, jm.fernandezvarea@ub.edu
(Dated: June 13, 2025)

Resum: L'objectiu d'aquest Treball de Final de Grau és estudiar dos models per a l'anàlisi quantitativa de la secció eficaç d'ionització de les capes internes. Hi ha dos models exposats en aquestes pàgines. El primer essent l'aproximació d'ona plana de Born (PWBA) i el segon és el model eCPSShsR, el qual millora l'anterior incloent les correccions de lligam, de Coulomb i de funció d'ona. Per a calcular els valors predits per la teoria, s'ha realitzat càlcul numèric per a blancs d'alumini, coure i plata i amb ions d'hidrogen i d'heli com a projectils amb energies des de 0.5 MeV fins a 20 MeV. La comparació de la corba teòrica amb els valors experimentals ha mostrat que el model eCPSShsR és el més acurat i que, per a energies del projectil grans, els models PWBA i eCPSShsR són pràcticament idèntics.
Paraules clau: secció eficaç, ionització, raigs X, apantallament, col·lisió inelàstica, correccions.
ODSs: Educació de qualitat. Indústria, innovació, infraestructures.

Objectius de Desenvolupament Sostenible (ODSs o SDGs)

1. Fi de la es desigualtats		10. Reducció de les desigualtats	
2. Fam zero		11. Ciutats i comunitats sostenibles	
3. Salut i benestar		12. Consum i producció responsables	
4. Educació de qualitat	X	13. Acció climàtica	
5. Igualtat de gènere		14. Vida submarina	
6. Aigua neta i sanejament		15. Vida terrestre	
7. Energia neta i sostenible		16. Pau, justícia i institucions sòlides	
8. Treball digne i creixement econòmic		17. Aliança pels objectius	
9. Indústria, innovació, infraestructures	X		

Bona part del contingut d'aquest TFG és part d'un grau universitari proporcionat per la Facultat de Física, per tant, s'inscriu en l'ODS 4, especialment a la fita 4.4, ja que recursos com aquest afavoreixen la divulgació de contingut tècnic a estudiants. També forma part de l'ODS 9, particularment de la fita 9.5, pel fet que s'analitzen les característiques d'un procés físic que té rellevància a la indústria i a la recerca.

GRAPHICAL ABSTRACT

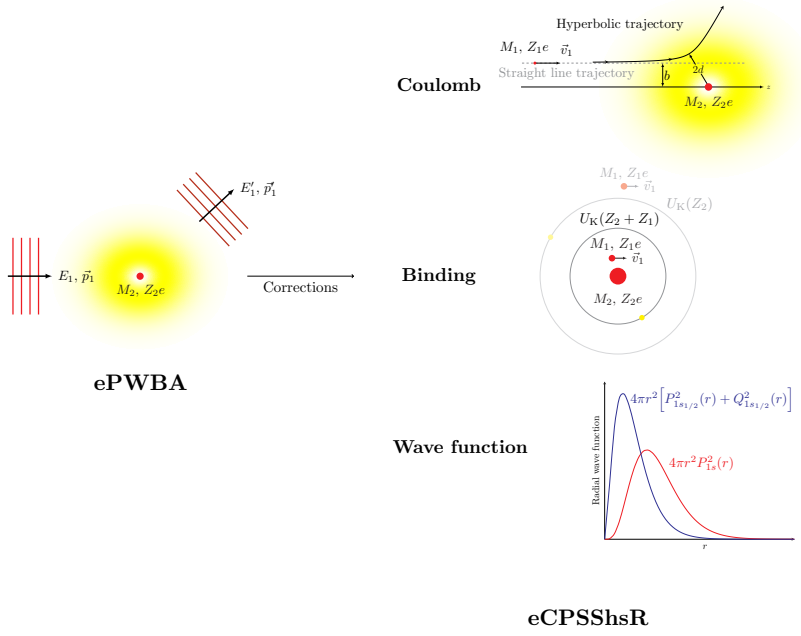

SUPPLEMENTARY MATERIAL

Appendix A: Hydrogenic GOS

It is customary to write the GOS in terms of the reduced variables

$$\mathcal{Q} \equiv \frac{Q}{Z_{2\mathrm{S}}^2 \mathcal{R}} \qquad \text{and} \qquad \mathcal{W} \equiv \frac{W}{Z_{2\mathrm{S}}^2 \mathcal{R}}, \tag{A1}$$

where $\mathcal{R} \equiv E_\mathrm{h}/2$ is the Rydberg energy. The S subindex means that the expression is valid for any shell. The reduced energy transfer is also related to the reduced wave number κ of the ionized electron in the final state

$$\mathcal{W} = \kappa^2 + \frac{1}{n^2}. \tag{A2}$$

The expression of the GOS pertaining to the hydrogenic (n, ℓ) (sub)shell is given by

$$\frac{\mathrm{d}f_{n\ell}(\mathcal{Q},\mathcal{W})}{\mathrm{d}\mathcal{W}} = A_n(\mathcal{Q},\mathcal{W})\, B_n(\mathcal{Q},\mathcal{W})\, C_{n\ell}(\mathcal{Q},\mathcal{W}), \tag{A3}$$

where the general expressions for the various factors can be found e.g. in the Appendix of Ref. [3]. In the particular case of the K shell ($n = 1$, $\ell = 0$) these coefficients are

$$A_1(\mathcal{Q},\mathcal{W}) = \begin{cases} 2^8\, \mathcal{W} \exp\left\{\left[-\frac{2}{\kappa} \arctan\left(\frac{2\kappa}{\mathcal{Q}-\mathcal{W}+2}\right)\right]\right\} f_\mathrm{C}(\kappa) & \text{if} \quad \kappa^2 > 0 \\ 2^8\, \mathcal{W} \exp\left\{\left[-\frac{1}{\sqrt{-\kappa^2}} \ln\left(\frac{\mathcal{Q}-\mathcal{W}+2+2\sqrt{-\kappa^2}}{\mathcal{Q}-\mathcal{W}+2-2\sqrt{-\kappa^2}}\right)\right]\right\} & \text{if} \quad \kappa^2 < 0 \end{cases} \tag{A4}$$

$$B_1(\mathcal{Q},\mathcal{W}) = \left[(\mathcal{Q}-\mathcal{W})^2 + 4\mathcal{Q}\right]^{-3} \tag{A5}$$

$$C_{10}(\mathcal{Q},\mathcal{W}) = \mathcal{Q} + \frac{\mathcal{W}}{3} \tag{A6}$$

with the Coulomb factor

$$f_\mathrm{C}(\kappa) = \left[1 - \exp\left(-\frac{2\pi}{\kappa}\right)\right]^{-1}. \tag{A7}$$

Appendix B: Derivation of the Coulomb correction factor

The proof will be presented for the general case and then particularized to the K shell. The SCA permits the derivation of the ionization differential cross sections for straight-line and hyperbolic trajectories of the projectile for slow collisions

$$\left(\frac{\mathrm{d}\sigma_\mathrm{S}}{\mathrm{d}E_f}\right)^{\mathrm{SCA,str}} \propto q_0^{-(\nu_\mathrm{S}+1)}\ , \tag{B1}$$

$$\left(\frac{\mathrm{d}\sigma_\mathrm{S}}{\mathrm{d}E_f}\right)^{\mathrm{SCA,hyp}} \propto \mathrm{e}^{-\pi d q_0/\hbar}\, q_0^{-(\nu_\mathrm{S}+1)}\ . \tag{B2}$$

Here $\nu_\mathrm{S} \equiv 9 + 2\ell$ and $q_0 \equiv (U_\mathrm{S} + E_f)/v_1 \equiv q_{0\mathrm{S}}\tau$ with $\tau = 1 + E_f/U_\mathrm{S}$. E_f is the kinetic energy of the ejected electron, thus $E_{f,\max} = E_1 - U_\mathrm{S}$. But for large Q values (low b values, where the correction is most important), $E_{f,\max} \approx E_1 \approx \infty$. Firstly, the ICSs for straight-line and hyperbolic trajectories are calculated,

$$\begin{aligned}\sigma_\mathrm{S}^{\mathrm{SCA,str}} &= \int_0^\infty \left(\frac{\mathrm{d}\sigma_\mathrm{S}}{\mathrm{d}E_f}\right)^{\mathrm{SCA,str}} \mathrm{d}E_f = A\int_0^\infty q_0^{-(\nu_\mathrm{S}+1)}\,\mathrm{d}E_f = \frac{A}{U_\mathrm{S}}\int_1^\infty q_0^{-(\nu_\mathrm{S}+1)}\,\mathrm{d}\tau \\ &= \frac{A}{U_\mathrm{S}}\left(\frac{U_\mathrm{S}}{v_1}\right)^{-(\nu_\mathrm{S}+1)}\int_1^\infty \tau^{-(\nu_\mathrm{S}+1)}\,\mathrm{d}\tau = \frac{1}{\nu_\mathrm{S}}\frac{A}{U_\mathrm{S}}\left(\frac{U_\mathrm{S}}{v_1}\right)^{-(\nu_\mathrm{S}+1)}\ .\end{aligned}$$

$$\sigma_{\mathrm{S}}^{\mathrm{SCA,hyp}} = \int_0^\infty \left(\frac{\mathrm{d}\sigma_{\mathrm{S}}}{\mathrm{d}E_f}\right)^{\mathrm{SCA,hyp}} \mathrm{d}E_f = A\int_0^\infty \mathrm{e}^{-\pi d q_0/\hbar}\, q_0^{-(\nu_{\mathrm{S}}+1)}\, \mathrm{d}E_f$$
$$= \frac{A}{U_{\mathrm{S}}}\left(\frac{U_{\mathrm{S}}}{v_1}\right)^{-(\nu_{\mathrm{S}}+1)} \int_1^\infty \mathrm{e}^{-\pi d q_{0\mathrm{S}}\tau/\hbar}\, \tau^{-(\nu_{\mathrm{S}}+1)}\, \mathrm{d}\tau = \frac{A}{U_{\mathrm{S}}}\left(\frac{U_{\mathrm{S}}}{v_1}\right)^{-(\nu_{\mathrm{S}}+1)} E_{\nu_{\mathrm{S}}+1}(\pi d q_{0\mathrm{S}}/\hbar)\ .$$

The Coulomb correction factor is finally,

$$C_{\mathrm{S}} \equiv \frac{\sigma_{\mathrm{S}}^{\mathrm{SCA,hyp}}}{\sigma_{\mathrm{S}}^{\mathrm{SCA,str}}} = \nu_{\mathrm{S}}\, E_{\nu_{\mathrm{S}}+1}(\pi d q_{0\mathrm{S}}/\hbar) \Rightarrow \boxed{C_{\mathrm{K}} = 9\, E_{10}(\pi d q_{0\mathrm{K}}/\hbar)}\ . \tag{B3}$$

Let it now obtain the expression for the d, half of the minimum distance between the projectile and the target nucleus when $b = 0$, that is, half of the value of the turning point: $d = r_0/2$. So, to know the expression it is only necessary to find the turning point.

The kinetic energy of the projectile in the laboratory frame is $E_1 = \frac{1}{2}M_1 v_1^2$ and the energy in the centre-of-mass reference frame is $E = \frac{1}{2}Mv^2$. Then, the effective potential energy is $U_{\mathrm{eff}}(r) = U(r) + \frac{L^2}{2Mr^2}$. Because there are no external forces and $b = 0$, then, we have $L = 0$ and $U(r) = Z_1 Z_2 e^2/r$. The turning point can be obtained when the total energy is equal to the potential energy,

$$\frac{1}{2}Mv_1^2 = \frac{Z_1 Z_2 e^2}{r_0} \Rightarrow r_0 = \frac{2Z_1 Z_2 e^2}{Mv_1^2} \Rightarrow \boxed{d = \frac{Z_1 Z_2 e^2}{Mv_1^2} = \frac{Z_1 Z_2 e^2}{2E} = \frac{Z_1 Z_2 e^2}{M}\frac{M_1}{2E_1}}\ . \tag{B4}$$

Appendix C: Derivation of the PSS correction

The main idea of this correction is that the lower limit of the integral over W will be shifted from U_{K} to $U_{\mathrm{K}} + \langle \Delta U_{\mathrm{K}} \rangle$. ΔU_{K} represents the increase in the binding energy caused by the presence of the projectile charge inside the electron cloud. Its expression can be obtained using 1st-order perturbation theory. The Hamiltonian of the perturbation is

$$\mathcal{H}' = -\frac{Z_1 e^2}{\left|\vec{\mathbf{r}} - \vec{\mathbf{R}}\right|}, \tag{C1}$$

where $\vec{\mathbf{r}}$ and $\vec{\mathbf{R}}$ are the positions of the electron and the projectile, respectively. Then, ΔU_{K} will be

$$\Delta U_{\mathrm{K}} = -\langle \psi_{100} | \mathcal{H}' | \psi_{100} \rangle\, . \tag{C2}$$

ψ_{100} is the hydrogenic wave function of the K-shell electrons, $\psi_{100}(\vec{\mathbf{r}}) = (P_{10}(r)/r)\, Y_{00}(\hat{\mathbf{r}})$. The negative sign appears because we are considering an increase in the binding energy. The matrix element is evaluated having recourse to the expansion

$$\frac{1}{\left|\vec{\mathbf{r}} - \vec{\mathbf{R}}\right|} = \sum_{\lambda=0}^{\infty}\sum_{\mu=-\lambda}^{\lambda} \frac{4\pi}{2\lambda+1}\frac{r_<^\lambda}{r_>^{\lambda+1}}\, Y_{\lambda\mu}^*(\hat{\mathbf{R}})\, Y_{\lambda\mu}(\hat{\mathbf{r}})\ , \tag{C3}$$

where $r_< = \min(r, R)$ and $r_> = \max(r, R)$. The expression then can be obtained following the next steps

$$\begin{aligned}
\langle\psi_{100}|\mathcal{H}'|\psi_{100}\rangle &= -Z_1 e^2 \int_{\mathbb{R}^3} \mathrm{d}^3\vec{\mathbf{r}}\; \psi^*_{100}(\vec{\mathbf{r}})\, \frac{1}{\left|\vec{\mathbf{r}} - \vec{\mathbf{R}}\right|}\, \psi_{100}(\vec{\mathbf{r}}) \\
&= -Z_1 e^2 \int_0^\infty \mathrm{d}r\; P^2_{10}(r) \int_{4\pi} \mathrm{d}\hat{\mathbf{r}}\; Y^*_{00}(\hat{\mathbf{r}}) \left[\sum_{\lambda=0}^{\infty}\sum_{\mu=-\lambda}^{\lambda} \frac{4\pi}{2\lambda+1}\, \frac{r_<^\lambda}{r_>^{\lambda+1}}\, Y^*_{\lambda\mu}\big(\hat{\mathbf{R}}\big)\, Y_{\lambda\mu}(\hat{\mathbf{r}})\right] Y_{00}(\hat{\mathbf{r}}) \\
&= -\frac{Z_1 e^2}{\sqrt{4\pi}} \sum_{\lambda=0}^{\infty}\sum_{\mu=-\lambda}^{\lambda} \frac{4\pi}{2\lambda+1}\, Y^*_{\lambda\mu}\big(\hat{\mathbf{R}}\big) \int_0^\infty \mathrm{d}r\; P^2_{10}(r)\, \frac{r_<^\lambda}{r_>^{\lambda+1}} \underbrace{\int_{4\pi} \mathrm{d}\hat{\mathbf{r}}\; Y^*_{00}(\hat{\mathbf{r}})\, Y_{\lambda\mu}(\hat{\mathbf{r}})}_{=\delta_{0\lambda}\,\delta_{0\mu}} \\
&= -Z_1 e^2 \int_0^\infty \mathrm{d}r\; \frac{P^2_{10}(r)}{r_>} \\
&= -Z_1 e^2 \left[\frac{1}{R}\int_0^R \mathrm{d}r\; P^2_{10}(r) + \int_R^\infty \mathrm{d}r\; \frac{P^2_{10}(r)}{r}\right] .
\end{aligned}$$

The radial integrals are

$$\begin{aligned}
\frac{1}{R}\int_0^R \mathrm{d}r\, P^2_{10}(r) &= \frac{4}{R}\left(\frac{Z_{2\mathrm{K}}}{a_0}\right)^3 \int_0^R \mathrm{d}r\, r^2 \exp\left(-\frac{2Z_{2\mathrm{K}} r}{a_0}\right) \\
&= \frac{1}{R}\left[1 - \exp\left(-\frac{2Z_{2\mathrm{K}}R}{a_0}\right)\left(1 + 2\frac{Z_{2\mathrm{K}}R}{a_0} + 2\left(\frac{Z_{2\mathrm{K}}R}{a_0}\right)^2\right)\right] , \qquad \text{(C4)} \\
\int_R^\infty \mathrm{d}r\, \frac{P^2_{10}(r)}{r} &= \left(\frac{2Z_{2\mathrm{K}}}{a_0}\right)^3 \int_R^\infty \mathrm{d}r\; r \exp\left(-\frac{2Z_{2\mathrm{K}} r}{a_0}\right) \\
&= \frac{1}{R}\exp\left(-\frac{2Z_{2\mathrm{K}}R}{a_0}\right)\left(2\left(\frac{Z_{2\mathrm{K}}R}{a_0}\right)^2 + \frac{Z_{2\mathrm{K}}R}{a_0}\right) , \qquad \text{(C5)}
\end{aligned}$$

where a_0 is the Bohr radius. Adding the two contributions we arrive at

$$\langle\psi_{100}|\mathcal{H}'|\psi_{100}\rangle = -\frac{Z_1 e^2}{R}\left[1 - \exp\left(-\frac{2Z_{2\mathrm{K}}R}{a_0}\right)\left(1 + \frac{Z_{2\mathrm{K}}R}{a_0}\right)\right] . \qquad \text{(C6)}$$

Finally, introducing the variable $y \equiv Z_{2\mathrm{K}}R/a_0$, the increase of the binding energy is

$$\boxed{\Delta U_{\mathrm{K}}(y) = Z_1 Z_{2\mathrm{K}} E_{\mathrm{h}}\, \frac{1}{y}\left[1 - \mathrm{e}^{-2y}(1+y)\right]} . \qquad \text{(C7)}$$

But, in order to obtain the proper limits of the integral for the PSS correction, the expression for the mean value should be calculated, $\langle\Delta U_{\mathrm{K}}\rangle$. It is important to remember the expression (7) so as to redefine the variable y: $y = \xi_{\mathrm{K}} x$. Then, the average increase in the binding energy is

$$\boxed{\langle\Delta U_{\mathrm{K}}\rangle = \int_0^{c_{\mathrm{K}}/\xi_{\mathrm{K}}} \Delta U_{\mathrm{K}}(\xi_{\mathrm{K}} x)\, w_{\mathrm{K}}(x)\; \mathrm{d}x} . \qquad \text{(C8)}$$

The weight factor $w_{\mathrm{K}}(x) = \frac{5}{32}x^4 K_2^2(x)$ can be derived within the SCA.

The limits of the integral of the mean value could have been extended from zero to infinity but that would have overestimated the correction. Instead, a better approach is to find the upper limit stating that the binding effect takes place when $b \lesssim \langle r\rangle_{\mathrm{K}}$, where $\langle r\rangle_{\mathrm{K}}$ is the mean radius of the K-shell. This constraint leads to the upper limit in Eq. (C8).

Appendix D: References with experimental data

H^+ on Al

[KP64] J. Khan, D. Potter. Characteristic K-shell X-ray production in magnesium, aluminum, and copper by 60- to 500-keV protons. *Physical Review*, 133(3A):A890–A894, 1964.

[KPW65] J. Khan, D. Potter, R. Worley. Studies in X-ray production by proton bombardment of C, Mg, Al, Nd, Sm, Gd, Tb, Dy, and Ho. *Physical Review*, 139(6A):A1735–A1746, 1965.

[BHV15] A.P.L. Bertol, R. Hinrichs, M.A.Z. Vasconcellos. Proton induced K X-ray production cross sections of the elements Al, Si, Ti, Fe, and Ni in the 0.7–2.0 MeV energy range. *Nuclear Instruments and Methods in Physics Research B*, 365:8–12, 2015.

[BBL73] G. Basbas, W. Brandt, R. Laubert. Universal cross sections for K-shell ionization by heavy charged particles. I. Low particle velocities. *Physical Review A*, 7(3):983–1001, 1973.

[Ser+80] K. Sera, K. Ishii, M. Kamiya, A. Kuwako, S. Morita. K-shell ionization of Al and Cu for 0.5–40-MeV-proton bombardment. *Physical Review A*, 21(5):1412–1418, 1980.

H^+ on Cu

[AJ74] R. Akselsson, T.B. Johansson. X-ray production by 1.5–11 MeV protons. *Zeitschrift für Physik*, 266:245–255, 1974.

[AME84] L. Avaldi, I. Mitchell, H. Eschbach. Precise X-ray production cross-section measurements of medium Z elements by protons. *Nuclear Instruments and Methods in Physics Research B*, 3(1-3):21–26, 1984.

[Bat+14] E. Batyrbekov, I. Gorlachev, I. Ivanov, A. Platov. K-, L- and M-shell x-ray production cross sections by 1–1.3 MeV protons. *Nuclear Instruments and Methods in Physics Research B*, 325:84–88, 2014.

[BG80] O. Benka, M. Geretschlager. K-shell ionisation cross sections for Ti, Fe, Cu, Zr and Ag by protons and He ions in the energy range 85–790 keV. *Journal of Physics B: Atomic and Molecular Physics*, 13(16):3223–3233, 1980.

[BM82] D. Bhattacharya, S. Mitra. K-shell ionisation cross-sections of Cu, Ge, Mo, Ag and Sn by protons of energy 0.3 to 1.8 MeV. *Pramana*, 19(4):399–412, 1982.

[Cip99] S.J. Cipolla. K X-ray production cross sections, K_β/K_α ratios, and radiative Auger ratios for protons impacting low-Z elements. *Nuclear Instruments and Methods in Physics Research A*, 422(1-3):546–550, 1999.

H^+ on Ag

[BM82] D. Bhattacharya, S. Mitra. K-shell ionisation cross-sections of Cu, Ge, Mo, Ag and Sn by protons of energy 0.3 to 1.8 MeV. *Pramana*, 19(4):399–412, 1982.

[BSW72] G. Bissinger, S. Shafroth, A. Waltner. Yields of K and L X rays arising from 2–30-MeV-proton bombardment of Ag. *Physical Review A*, 5(5):2046–2052, 1972.

[LAH80] E. Laegsgaard, J.U. Andersen, F. Høgedal. Accurate determination of cross sections for K-shell ionization by proton impact. *Nuclear Instruments and Methods*, 169(2):293–300, 1980.

He^{2+} on Al

[BBL73] G. Basbas, W. Brandt, R. Laubert. Universal cross sections for K-shell ionization by heavy charged particles. I. Low particle velocities. *Physical Review A*, 7(3):983–1001, 1973.

[Dup+11] T. Dupuis, G. Chere, P. Mathis, A. Marchal, H.-P. Garnir, D. Strivay. X-ray production cross-sections measurements for high-energy alpha particle beams: New dedicated set-up and first results with aluminium. *Nuclear Instruments and Methods in Physics Research B*, 269(24):2979–2983, 2011.